






Clinisys

**GLIMS Genetics**

**clinisys**

Enabling healthier communities

# A recurrent de novo variant in *NUSAP1* escapes nonsense-mediated decay and leads to microcephaly, epilepsy, and developmental delay

Alisa Mo<sup>1</sup> | Emuna Paz-Ebstein<sup>2,3</sup> | Shira Yanovsky-Dagan<sup>2</sup> | Abbe Lai<sup>4</sup> |  
Hagar Mor-Shaked<sup>2,3</sup> | Tal Gilboa<sup>3,5</sup>  | Edward Yang<sup>6</sup> | Diane D. Shao<sup>1</sup>  |  
Christopher A. Walsh<sup>4,7</sup> | Tamar Harel<sup>2,3</sup> 

<sup>1</sup>Department of Neurology, Boston Children's Hospital, Harvard Medical School, Boston, Massachusetts, USA

<sup>2</sup>Department of Genetics, Hadassah Medical Center, Jerusalem, Israel

<sup>3</sup>Faculty of Medicine, Hebrew University of Jerusalem, Jerusalem, Israel

<sup>4</sup>Division of Genetics and Genomics, Department of Pediatrics, Boston Children's Hospital, Boston, Massachusetts, USA

<sup>5</sup>Pediatric Neurology Unit, Hadassah Medical Center, Jerusalem, Israel

<sup>6</sup>Department of Radiology, Boston Children's Hospital, Boston, Massachusetts, USA

<sup>7</sup>Howard Hughes Medical Institute, Boston Children's Hospital, Boston, Massachusetts, USA

## Correspondence

Tamar Harel, Department of Genetics,  
Hadassah-Hebrew University Medical Center,  
POB 12000, Jerusalem, Israel 9112001.  
Email: [tamarhe@hadassah.org.il](mailto:tamarhe@hadassah.org.il)

## Funding information

Joint Research Fund (Keren Meshutefet) of the Hebrew University and Hadassah and Shaare Zedek Hospitals; National Eye Institute; National Heart, Lung, and Blood Institute, Grant/Award Number: UM1 HG008900; National Human Genome Research Institute, Grant/Award Number: R01 HG009141; National Institute of Neurological Disorders and Stroke, Grant/Award Number: R01NS035129; NIH/NICHD K12 HD052806; NIH/NINDS R25 NS070682

## Abstract

*NUSAP1* encodes a cell cycle-dependent protein with key roles in mitotic progression, spindle formation, and microtubule stability. Both over- and under-expression of *NUSAP1* lead to dysregulation of mitosis and impaired cell proliferation. Through exome sequencing and Matchmaker Exchange, we identified two unrelated individuals with the same recurrent, de novo heterozygous variant (NM\_016359.5 c.1209C > A; p.(Tyr403Ter)) in *NUSAP1*. Both individuals had microcephaly, severe developmental delay, brain abnormalities, and seizures. The gene is predicted to be tolerant of heterozygous loss-of-function mutations, and we show that the mutant transcript escapes nonsense mediated decay, suggesting that the mechanism is likely dominant-negative or toxic gain of function. Single-cell RNA-sequencing of an affected individual's post-mortem brain tissue indicated that the *NUSAP1* mutant brain contains all main cell lineages, and that the microcephaly could not be attributed to loss of a specific cell type. We hypothesize that pathogenic variants in *NUSAP1* lead to microcephaly possibly by an underlying defect in neural progenitor cells.

## KEYWORDS

exome sequencing, mendelian genetics, microcephaly, nonsense mediated decay, *NUSAP1*

Alisa Mo, Emuna Paz-Ebstein, and Tamar Harel contributed equally to this work.

This is an open access article under the terms of the [Creative Commons Attribution-NonCommercial-NoDerivs](https://creativecommons.org/licenses/by-nc-nd/4.0/) License, which permits use and distribution in any medium, provided the original work is properly cited, the use is non-commercial and no modifications or adaptations are made.

© 2023 The Authors. *Clinical Genetics* published by John Wiley & Sons Ltd.

## 1 | INTRODUCTION

Primary microcephaly, defined as a head circumference less than three standard deviations below the population mean, is accompanied by varying degrees of cognitive deficiency and developmental delay. Proper cortical development is dependent upon a balance between symmetric proliferative divisions generating additional progenitors, versus asymmetric divisions resulting in neuronal differentiation. Dysregulation of mitosis in neural progenitors, resulting in excessive apoptosis or precocious differentiation, disrupts this balance and leads to a decrease in the neural progenitor pool, resulting in microcephaly.<sup>1</sup> Accordingly, monogenic causes underlying primary microcephaly mostly converge on genes that encode proteins associated with cell division such as centriole biogenesis and assembly (*ASPM*, *CDK5RAP2*, *CENPJ*, *CEP135*, *CEP152*, *WDR62*) and kinetochore assembly and function (*CASC5*, *CENPE*). Less commonly perturbed pathways include DNA repair (*ATR*, *DONSON*, *MCPH1*, *PNKP*), Wnt signaling (*WDFY3/ALFY*), and amino acid or protein synthesis (*AARS*, *QARS*).<sup>2,3</sup>

*NUSAP1* encodes Nuclear and Spindle Associated Protein (*NUSAP1*), a cell cycle-dependent protein selectively expressed in proliferating cells, including in the brain. It has key roles in mitotic progression, spindle formation, and microtubule stability. The expression and protein abundance of *NUSAP1* peak in the G2 and M phases of the cell cycle and sharply decrease at mitotic exit. At mitotic onset, *NUSAP1* accumulates at the growing ends of kinetochore microtubules and stabilizes them by negatively regulating the mitotic centromere-associated kinesin (*MCAK*) microtubule depolymerising activity.<sup>4–6</sup> Both *NUSAP1* depletion by RNA interference and *NUSAP1* overexpression lead to dysregulation of mitosis and impaired cell proliferation.<sup>4,7</sup>

In this study, we report two unrelated individuals with congenital microcephaly, epilepsy, severe developmental delay, and brain abnormalities, found to have a common de novo heterozygous nonsense variant in *NUSAP1*. We provide detailed clinical descriptions and in vitro evidence that the mutant *NUSAP1* escapes nonsense mediated decay (NMD) and review the relevant literature supporting a critical role of *NUSAP1* in neuronal proliferation.

## 2 | MATERIALS AND METHODS

### 2.1 | Ethics statement

Research performed on samples of human origin was conducted in accordance with the ethical standards of the responsible national and institutional committees on human subject research at Boston Children's Hospital and Hadassah Medical Center.

### 2.2 | Exome analysis

For family A, following informed consent, exome analysis was performed on DNA extracted from whole blood of the proband and his

parents. Exonic sequences from DNA were enriched with the SureSelect Human All Exon 50 Mb V5 Kit (Agilent Technologies, Santa Clara, California, USA). Sequences were generated on a HiSeq2500 system (Illumina, San Diego, California, USA) as 125 bp paired-end runs. Read alignment and variant calling were performed with DNAnexus (Palo Alto, California, USA) using default parameters with the human genome assembly hg19 (GRCh37) as reference. Exome analysis of the proband yielded 81.5 million reads, with a mean coverage of 123X. Following alignment to the reference genome [hg19] and variant calling, variants were filtered out if they were off-target (>8 bp from splice junction), synonymous, or had minor allele frequency >0.5% in the gnomAD database.

For Family B, exome sequencing and data processing were done at the Genomics Platform at the Broad Institute of MIT and Harvard. An exome sequencing library was generated using the Illumina Nextera exome capture kit and sequenced using 150 bp paired-end reads to cover >80% of targets at 20X coverage and a mean target coverage of >100X. Exome sequencing data were processed using the standard pipeline with Picard. *BWA*<sup>8</sup> was used to align reads to hg38, and SNV and insertions/deletions were called using GATK HaplotypeCaller<sup>9</sup> using default filters. Variants were annotated using Variant Effect Predictor and uploaded to Seqr<sup>10</sup> for further review. Hg19 coordinates in Seqr were used to facilitate comparison with Family A.

### 2.3 | Sanger validation and segregation of the variant

For both families, the *NUSAP1* variant was confirmed via Sanger sequencing of the affected individual and compared to the phenotypically normal parents.

### 2.4 | Cell culture and generation of cell lines

Primary fibroblasts were grown from skin-punch biopsies and maintained in Dulbecco's modified Eagle's medium (DMEM) supplemented with 15% FCS, 1% L-glutamine, and 1% penicillin-streptomycin antibiotics (Biological Industries Beit Haemek, Israel). Lymphoblastoid cell lines (LCLs) were generated by EBV-transformation and maintained in Roswell Park Memorial Institute (RPMI)-1640 supplemented with 20% FCS, 1% L-glutamine, and 1% penicillin-streptomycin antibiotics (Biological Industries Beit Haemek, Israel).

### 2.5 | cDNA analysis

Total RNA was isolated from fresh lymphocytes, EBV-transformed LCLs, and cultured fibroblasts of the affected individual in Family A and from control individuals by TRIzol reagent extraction. cDNA was reverse transcribed from 1 µg RNA using the qScript cDNA Synthesis

Kit (Quantabio) which included Oligo (dT) and random primers. The region encompassing exons 9–11 of *NUSAP1* was amplified by PCR using PCR BIO HS Taq Mix Red (PCR BIOSYSTEMS) with the following primers: NUSAP1\_RNA\_F1: 5'-AGTTTGTCTCGTCCCCTCAA-3', NUSAP1\_RNA\_R1: 5'-CGTTTCTTCCGTTGCTCTTC-3'. *ACTB* served as a loading control and was amplified with the following primers: act\_b\_F: 5'-GATCAAGATCATTGCTCCTC-3' and act\_b\_R: 5'-TTGTCAAGAAAGGGTGTAAC-3'. The region encompassing exons 9–11 of *NUSAP1* was also quantified by real-time qPCR using PerfeCTa SYBR Green FastMix ROX (Quantabio) in the StepOnePlus Real-Time PCR system (Thermo Fisher) with the following primers: NUSAP1\_RNA\_F2: 5'-TTTGTCTCGTCCCCTCAACT-3' and NUSAP1\_RNA\_R2: 5'-TTCCAAAACCTTTGCTTTC-3'. *HPRT1* served as a loading control (HPRT1\_F: 5'-TGACACTGGCAAACAATGCA-3' and HPRT1\_R: 5'-GGTCTTTTACCAGCAAGCT-3'). The qPCR experiments were done in triplicates on three independent biological replicates. Allele-specific RT-PCR was performed using a nonspecific forward primer (NUSAP1\_AS\_F1: 5'-ACAACCTGAGGCAACGCAGAC-3') and a specific reverse primer (NUSAP1\_AS\_R1: 5'-TGGAGATGGGGTTGTTT-3').

## 2.6 | Single-cell RNA-seq of postmortem *NUSAP1* brain

For single-cell RNA-seq (scRNA-seq), a sample of post-mortem fresh-frozen prefrontal cortex from Family B, Individual II-1 was Dounce homogenized to release nuclei. Ten thousand single nuclei were isolated using fluorescence-activated nuclei sorting for capture on the 10X Genomics Chromium controller according to the Chromium Next GEM Single Cell 3' Reagent Kit v3.1 (dual index) user guide (10X Genomics). Library preparation was performed according to the manufacturer's protocol and sequenced on the Illumina NovaSeq 6000 with paired-end 150 bp reads for a total of 419 million reads. Age- and sex-matched control prefrontal cortex scRNA-seq data was downloaded from Sequence Read Archive (accession PRJNA434002) for brain ID 5408 in Velmeshev et al., 2019.<sup>11</sup> For both samples, raw reads were preprocessed using cellranger v.5.0.0,<sup>12</sup> and the cellranger count function was used to generate per-cell gene expression matrices by aligning the reads to the GRCh38-1.2.0 transcriptome (Ensembl release 84). scRNA-seq data was analyzed using the R package Seurat (v4.1.1).<sup>13</sup> Briefly, the expression matrices of both samples were filtered, merged into a Seurat object, normalized, and log-transformed. Anchors across the two datasets were identified using reciprocal principal component analysis (PCA) by running PCA on each dataset before integration, and then using the FindIntegrationAnchors function. The two datasets were integrated with IntegrateData, and clustering was performed (ScaleData, RunPCA, RunUMAP, FindNeighbors, and FindClusters) and visualized using Uniform Manifold Approximation and Projection (UMAP) reduction. The identity of each cluster was then manually annotated based on expression of known marker genes from previously published scRNA-seq datasets.<sup>14</sup>

## 3 | RESULTS

### 3.1 | Clinical reports

#### 3.1.1 | Family A

The proband (Figure 1A, Family A, individual II-2) was a 4-year and 11-month-old male with severe global developmental delay, microcephaly, and epilepsy (Table 1). He was the second of three children born to nonconsanguineous parents of Arab-Muslim descent. Parental ages at birth were 22 (mother) and 26 (father). Family history was negative. Prenatal ultrasound showed microcephaly and agenesis of the corpus callosum. Measurements of the cerebellum, pons, and vermis were all below the third percentile. Fetal echocardiogram was normal. The child was born at 40 2/7 weeks with a birthweight of 3010 grams (24th %ile) and a head circumference of 30.5 cm (Z score=−3.31). Apgar scores were 9 at 1 min and 10 at 5 min. He had neonatal seizures which were controlled with phenobarbital. Physical exam showed a small forehead, prominent nose, high palate, and small chin. The child had global developmental delay; at age 4 years and 11 months, he was unable to support his head, and he had no verbal or nonverbal communication skills. He had axial and peripheral hypotonia as well as cortical visual impairment (CVI). He developed three seizure semiologies, including generalized tonic-clonic seizures, asymmetric spasms, and myoclonic seizures. His epilepsy was refractory; treatment at time of last evaluation included vigabatrin, sodium valproate, and ketogenic diet, but he continued to have breakthrough seizures in the setting of febrile illness. Prior anti-seizure medications included phenobarbital, levetiracetam, and topiramate. Video electroencephalogram at 3 years of age showed generalized background slowing and multifocal as well as generalized interictal epileptiform discharges. EEG captured myoclonic seizures, asymmetric spasms, and electrographic seizures. Brain MRI at age 1.5 months revealed microcephaly, gyral simplification, a rudimentary corpus callosum, olfactory bulb hypoplasia, nearly absent midline commissures, and sub-ependymal nodules in the lateral ventricles. Subsequent MRI at 28 months of age was stable with no progression (Figure 2A–D). He had a feeding gastrostomy tube and Nissen fundoplication due to recurrent aspiration pneumonia. At night, breathing was supported by a BiPAP machine. Hearing evaluation was normal. Metabolic and infectious work-up were negative. Genetic work-up included chromosomal microarray which did not detect pathogenic or likely pathogenic copy number variants, and trio exome sequencing was pursued in order to identify the underlying molecular diagnosis.

#### 3.1.2 | Family B

In Family B, the proband (Figure 1A, Family B, individual II-1) was a Caucasian male with severe microcephaly, global developmental delay, and epilepsy. Family history was negative, and there was no known consanguinity. Prenatal ultrasound and fetal MRIs showed

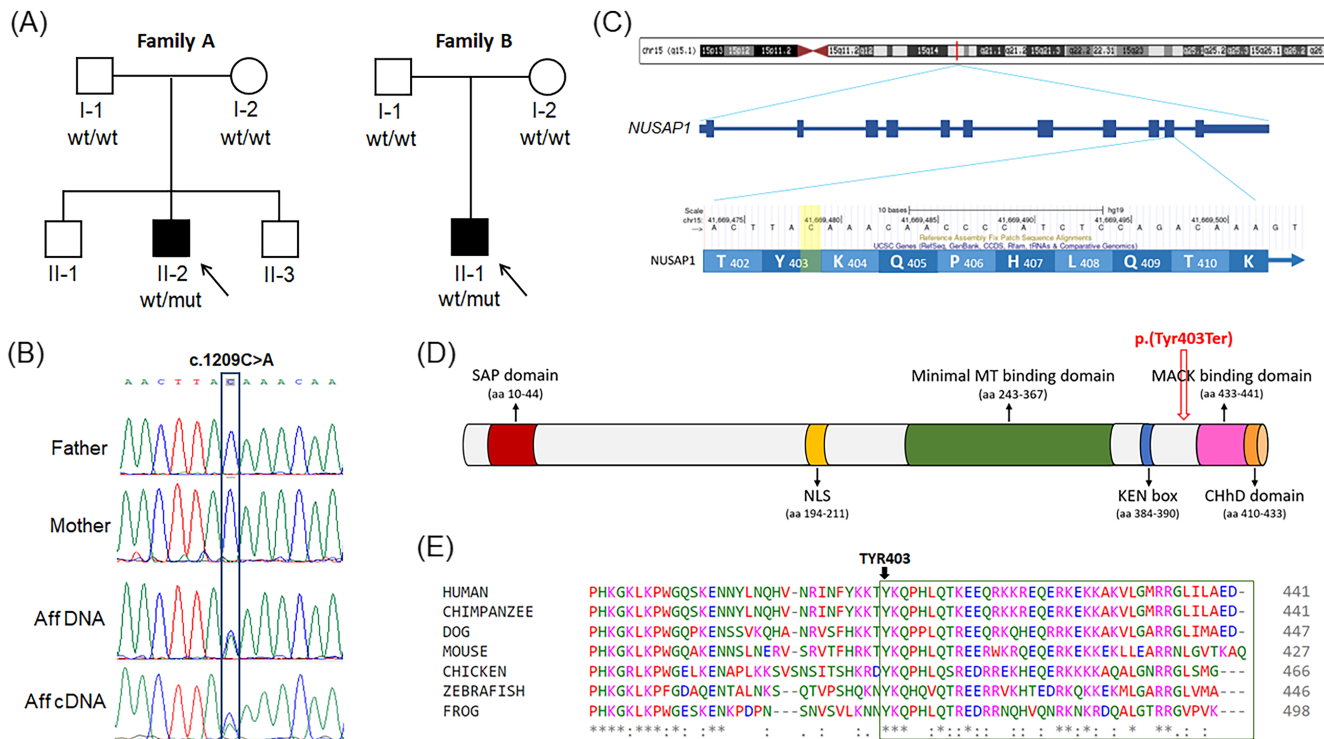


**FIGURE 1** Pedigrees, Sanger sequencing, and schematic figures of the *NUSAP1* gene and protein. (A) Pedigrees of both families showing the de novo variant in affected individuals. (B) Sanger sequencing in Family A shows wild-type traces in both parents and the heterozygous variant in the affected individual II-2. The bottom trace shows that both alleles are present in the cDNA. (C) Schematic representation of *NUSAP1*, showing that the variant is located within the last 50 bp of the penultimate exon. (D) Schematic representation of the *NUSAP1* protein. The mutant protein is expected to lose the MACK binding domain and the CHhD domain. (E) Inter-species conservation of the C-terminal domain.

microcephaly and an inter-hemispheric cyst. The child was born at term with a birthweight of 2819 g (13th %ile). Head circumference was unknown at birth and 34 cm at 3 months of age (<5th %ile). He developed seizures starting from the first day of life and ultimately had frequent clusters of focal clonic and generalized tonic-clonic seizures that were medically refractory to levetiracetam, phenobarbital, clonazepam, and topiramate. The affected individual had a social smile but was nonverbal and could not sit or roll over. He had CVI and hearing impairment. Exam was notable for dysmorphic facial features including hypertelorism, forehead abnormality, flat face, upslanting palpebral fissures and anteverted nares, truncal hypotonia, and lower extremity spasticity with clonus and mild contractures (Table 1). Interictal EEG showed multifocal spike waves and diffuse background slowing. Brain MRI (Figure 2E–H) showed microcephaly, partial agenesis of the corpus callosum, gyral abnormalities, and other brain abnormalities (Table 1). He required gastrostomy tube placement. He had recurrent respiratory infections and required BiPAP. He ultimately died at 3 years and 3 months of age due to complications of a respiratory infection. Neuropathological characterization of the postmortem brain tissue also showed severe microcephaly (brain weight 440 grams compared with normal for age 1270 g ± 210 g), arhinencephaly, partial agenesis of the corpus callosum, multiple cortical gyral abnormalities, poorly laminated cerebral cortex, multiple periventricular, deep white matter, and cerebellar neuronal heterotopia, poorly infolded hippocampi, and

small internal capsules. Trio whole exome sequencing was performed to identify an underlying molecular diagnosis.

### 3.2 | De novo variant in *NUSAP1* identified in both probands

Exome sequencing in each proband identified an identical heterozygous stopgain variant in *NUSAP1*: chr15:41669479C > A [hg19]; NM\_016359.5; c.1209C > A; p.(Tyr403Ter), which was de novo in each affected individual. Following filtering of exome sequencing data, no pathogenic or likely pathogenic variants were identified in genes previously associated with microcephaly. Read-depth analysis did not reveal any pathogenic or likely pathogenic copy number variants. The variant in *NUSAP1* was not found in gnomAD or local databases. Sanger sequencing validated the variant in the probands and its absence in the unaffected parents (Figure 1B). Other variants of interest after filtering of the exome data are provided in Table S1. A hemizygous missense variant was identified in *HCFC1*. However, the variant had a low GERP score and conflicting bioinformatic predictions. The clinical presentation was not suggestive of the disorder—newborn screening was normal and the child did not have any episodes of metabolic decompensation. Therefore, the variant was not considered pathogenic or likely pathogenic.

**TABLE 1** Clinical features.

	Family A, Individual II-2	Family B, Individual II-1
Age at last evaluation	4 years 11 months	3 years 1 months (died at 3 years 3 months due to respiratory infection)
Gender	Male	Male
Prenatal ultrasound	Microcephaly, agenesis of the CC, small hindbrain	Microcephaly, inter-hemispheric cyst
Gestational age	40 2/7 weeks	Full-term
Birthweight	3010 g	2819 g
Head circumference at birth	30.5 (Z score−3.31)	Unknown, 34 cm at 3 months of age (<5%ile)
Developmental delay	Severe	Severe (nonverbal)
Hypotonia	+	Truncal hypotonia, lower extremity spasticity with clonus and contractures
Epilepsy	+	+
Brain MRI/Autopsy neuropathology	Microcephaly, gyral simplification, bilateral periventricular nodular heterotopia, rudimentary CC, nearly absent midline commissures, olfactory bulb hypoplasia, interhemispheric cyst, intrahypothalamic adhesions, small mamillary bodies, nonspecific T2 hyperintensities in posterior cortical white matter	Microcephaly, gyral simplification, partial agenesis of the CC, periventricular and deep white matter heterotopias, poorly laminated cerebral cortex with numerous subcortical heterotopic neurons and pallor of myelin staining, occipital cortex with focal polymicrogyric-like appearance, aplasia of the olfactory bulbs and tracts, leptomeningeal glioneuronal heterotopias, irregular shape of putamen and globus pallidus, poorly folded hippocampi, interhemispheric cyst, cerebellar heterotopias
Visual disturbances	CVI	CVI
Feeding gastrostomy	+	+
Respiratory difficulties	+ (BiPAP at night)	+ (BiPAP at night)
Hearing impairments	−	+
Dysmorphic features	Small forehead, prominent nose, high palate, small chin	Hypertelorism, forehead abnormality, flat face, upslanting palpebral fissures, anteverted nares, abnormal palmar creases
Other	Negative metabolic and infectious work-up	−
Chromosomal microarray/FISH	Normal chromosomal microarray	Normal subtelomere FISH
Exome sequencing	<i>NUSAP1</i> (NM_016359.5): c.1209C > A; p.(Tyr403Ter)	<i>NUSAP1</i> (NM_016359.5): c.1209C > A; p.(Tyr403Ter)

Abbreviations: CC, corpus callosum; CVI, cortical visual impairment; FISH, fluorescence in situ hybridization.

### 3.3 | Core clinical phenotype of *NUSAP1*-affected individuals

The connection between the two cases was facilitated by GeneMatcher.<sup>15</sup> Common core features of the two cases are microcephaly, gyral simplification, heterotopic neurons, and defects in midline structures including partial agenesis of the corpus callosum and olfactory bulb hypoplasia. Clinically, both individuals had severe global developmental delay, hypotonia, epilepsy, and cortical visual impairment.

### 3.4 | Mutant transcript escapes nonsense mediated decay

The *NUSAP1* variant is expected to lead to a premature truncation codon within the last 50 base pairs of the penultimate exon (Figure 1C), and is thus predicted to escape NMD.<sup>16,17</sup> The probability of loss of function intolerance (pLI) score of the gene is 0.05, with an

observed/expected (o/e) ratio of 0.3.<sup>18</sup> The vast majority of the predicted loss-of-function variants in gnomAD are located upstream of this variant. To determine whether the mutant transcript triggers or escapes NMD, we sequenced the cDNA from LCLs and showed that peaks of both transcripts were present (Figure 1B). Semi-quantitative RT-PCR on cDNA derived from whole blood, LCLs, and fibroblasts, and qPCR on cDNA from patient and control fibroblasts showed that *NUSAP1* expression level was comparable to that of controls (Figure S1). Allele-specific RT-PCR showed strong expression of the mutant allele only in the patient sample (Figure S2). Collectively, the data indicate that the mutant transcript escapes NMD. Protein analysis in transfected HEK293 cells of wild type and mutant *NUSAP1* also confirmed the formation of a truncated protein (data not shown). *NUSAP1* is a ~55 kDa protein with mostly alpha-helices and coils as well as short stretches of extended beta-sheets.<sup>4</sup> The mutant p-Tyr403Ter is expected to lack its C-terminus (Figure 1D), which includes a charged helical domain (ChHD) (aa 410–433) and the mitotic centromere-associated kinesin (MCAK)-binding domain

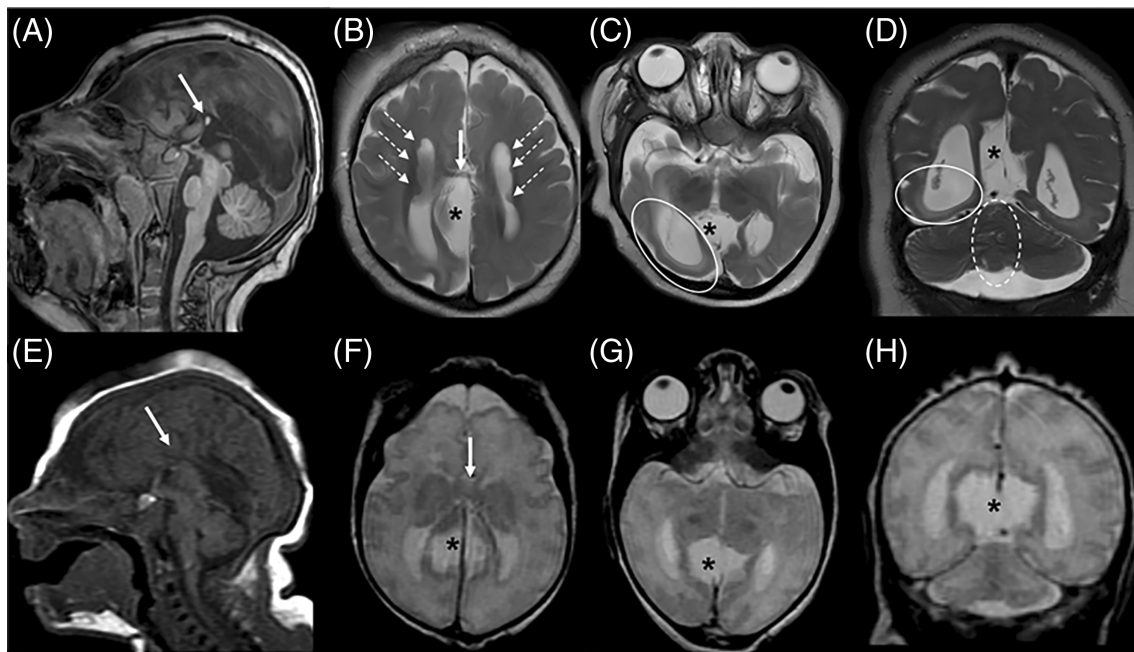


**FIGURE 2** Brain MRIs of subjects Family A, individual II-2 (A–D) at 2 years of life and Family B, individual II-1 (E–H) at 3 days of life demonstrate common features. Sagittal T1 (A, E), axial T2 (B, C, F, G), and coronal T2 (D, H) images demonstrate sloping of the forehead consistent with microcephaly, callosal dysgenesis with only minimal commissural tissue (arrows with solid stems, A, B and E, F) with associated dysmorphology of the lateral ventricles (parallel configuration, colpocephaly), and a midline CSF clearing consistent with an interhemispheric cyst (asterisks, B–D and F–H). The higher resolution images available for Family A, individual II-2 additionally demonstrate subependymal gray matter heterotopia (arrows with dashed stems, B), posterior quadrant T2 hyperintensity consistent with dysmyelination, regional microlissencephaly of the right temporo-occipital lobe (circle, C and D), and distortion of cerebellar folia at the midline (dashed circle, D).

(aa 433–441).<sup>4,7,19</sup> We, therefore, hypothesized that the variant results in a truncated protein, lacking the conserved C-terminal region (Figure 1D,E), which would exert a pathogenic effect via a dominant negative or gain of function mechanism.

### 3.5 | NUSAP1 mutant brain contains all major cell lineages

As NUSAP1 is selectively expressed early in brain development in dividing progenitor cells,<sup>4</sup> we predicted that the NUSAP1 mutant brain would contain all major cell lineages. We performed scRNA-seq on the post-mortem fresh-frozen prefrontal cortex from Family B, individual II-1 and were able to detect upper and lower layer excitatory neurons, three main categories of inhibitory neurons, astrocytes, oligodendrocytes, oligodendrocyte progenitor cells, and microglia (Figure S3A). We further confirmed that NUSAP1 is not expressed in either mutant or control post-natal brain (Figure S3B).

## 4 | DISCUSSION

In this study, we have identified a recurrent de novo pathogenic variant in NUSAP1 in two unrelated affected individuals as a cause of microcephaly. The affected individuals present with phenotypes of

severe developmental delay, tone abnormalities, and epilepsy, and show common brain abnormalities including microcephaly, underdevelopment of midline structures, and periventricular heterotopia. Overall, identification of a pathogenic variant in NUSAP1 adds a novel gene involved in cell division to our understanding of the genetic basis of microcephaly.

The mRNA and protein levels of NUSAP1 peak at the transition of G2 to mitosis and decline rapidly following cell division,<sup>4</sup> indicating tight regulation throughout the cell cycle. Both under- and overexpression of NUSAP1 lead to abnormalities in spindle organization and bundling of spindle microtubules.<sup>4,6</sup> *Nusap1*-null embryos in a murine model die by embryonic day 10.5, with severe abnormalities in spindle organization, chromosome congression, and chromosome alignment,<sup>6</sup> and morpholino studies in zebrafish demonstrated that *nusap1* morphants display impaired morphogenesis and defective migration of neural crest cells. Injection of *nusap1* mRNA alone caused apoptosis in the eyes and hindbrain, further suggesting in vivo significance of the gene in cell cycle progression.<sup>20</sup>

The variant in NUSAP1 is located in the penultimate exon of a gene predicted to be generally tolerant of heterozygous loss-of-function mutations, and the mutant transcript escapes NMD. NUSAP1 stabilizes kinetochore microtubules through negative regulation of the MCAK depolymerizing activity, thus decreasing the turnover rate of kinetochore microtubules during metaphase.<sup>21,22</sup> The truncated p-Tyr403Ter protein lacking the MCAK-binding domain is predicted to

perturb kinetochore microtubule dynamics. As NUSAP1 expression is restricted to mitotically active cells, including in the fetal developing brain,<sup>6</sup> we hypothesize that the disturbance of the MCAK-binding domain in the NUSAP1 p.Tyr403Ter brain is a potential mechanism to explain the microcephaly phenotype. Further studies are required to determine whether the variant exerts its pathogenic effect via a dominant-negative or gain-of-function mechanism.<sup>17,23</sup>

Consistent with the exclusive expression of NUSAP1 in progenitor cells and an early defect in neurogenesis, our scRNA-seq data shows that the NUSAP1 mutant brain contains all of the major cell lineages in the brain. However, given the relatively low numbers of single cells analyzed, differences in dissecting techniques, and the “n of 1” NUSAP1 mutant brain, we cannot determine whether the NUSAP1 brain contains all rare cell subpopulations or whether there are differences in cell type abundance. The NUSAP1 brain also showed increased expression of pro-inflammatory genes compared to the control brain (data not shown), but this result may be an artifact of differences in post-mortem tissue collection and sample processing.

In conclusion, we have identified a recurrent de novo variant in NUSAP1 causing microcephaly, underdevelopment of midline brain structures, developmental delay, and epilepsy. We show that NUSAP1 escapes NMD and is therefore predicted to function as a dominant-negative or gain-of-function allele. Further studies are needed to define the full clinical spectrum of NUSAP1-related microcephaly, the correlation between genotype and phenotype, and the mechanism of disease.

#### AUTHOR CONTRIBUTIONS

Alisa Mo, Abbe Lai, Diane D. Shao, Tal Gilboa, and Tamar Harel collected clinical data and analyzed genomic data. Alisa Mo, Emuna Paz-Ebstein, Shira Yanovsky-Dagan, and Diane D. Shao performed molecular experiments. Edward Yang reviewed and interpreted imaging results. Hagar Mor-Shaked analyzed exome sequencing data. Alisa Mo, Emuna Paz-Ebstein, Shira Yanovsky-Dagan, Diane D. Shao, Christopher A. Walsh, and Tamar Harel interpreted data and wrote the manuscript. All authors edited and approved the final version.

#### ACKNOWLEDGMENTS

The authors thank the families for their participation in this study. AM and DDS received support from the NIH/NINDS R25 NS070682. DDS also received support from NIH/NICHD K12 HD052806. Sequencing and analysis were provided by the Broad Institute of MIT and Harvard Center for Mendelian Genomics (Broad CMG) and was funded by the National Human Genome Research Institute, the National Eye Institute, and the National Heart, Lung and Blood Institute grant UM1 HG008900 and in part by National Human Genome Research Institute grant R01 HG009141. CAW is supported by a grant from the National Institute of Neurological Disorders and Stroke (R01NS035129) and is an Investigator of the Howard Hughes Medical Institute. TH received research support from the Joint Research Fund (Keren Meshutefet) of the Hebrew University and Hadassah and Shaare Zedek Hospitals.

#### CONFLICT OF INTEREST STATEMENT

The authors have declared that no conflict of interest exists.

#### PEER REVIEW

The peer review history for this article is available at <https://www.webofscience.com/api/gateway/wos/peer-review/10.1111/cge.14335>.

#### DATA AVAILABILITY STATEMENT

The ClinVar accession number for the DNA variant data is SCV002526432.

#### ORCID

Tal Gilboa  <https://orcid.org/0000-0003-3060-422X>

Diane D. Shao  <https://orcid.org/0000-0003-2087-4082>

Tamar Harel  <https://orcid.org/0000-0003-3595-7075>

#### REFERENCES

- Mitchell-Dick A, Chalem A, Pilaz LJ, Silver DL. Acute lengthening of progenitor mitosis influences progeny fate during cortical development in vivo. *Dev Neurosci*. 2019;41(5–6):300–317. doi:10.1159/000507113
- Degrassi F, Damizia M, Lavia P. The mitotic apparatus and kinetochores in microcephaly and neurodevelopmental diseases. *Cells*. 2019;9(1):49. doi:10.3390/cells9010049
- Jayaraman D, Bae BI, Walsh CA. The genetics of primary microcephaly. *Annu Rev Genomics Hum Genet*. 2018;08(19):177–200. doi:10.1146/annurev-genom-083117-021441
- Raemaekers T, Ribbeck K, Beaudouin J, et al. NuSAP, a novel microtubule-associated protein involved in mitotic spindle organization. *J Cell Biol*. 2003;162(6):1017–1029. doi:10.1083/jcb.200302129
- Ribbeck K, Groen AC, Santarella R, et al. NuSAP, a mitotic RanGTP target that stabilizes and cross-links microtubules. *Mol Biol Cell*. 2006;17(6):2646–2660. doi:10.1091/mbc.e05-12-1178
- Vanden Bosch A, Raemaekers T, Denayer S, et al. NuSAP is essential for chromatin-induced spindle formation during early embryogenesis. *J Cell Sci*. 2010;123(Pt 19):3244–3255. doi:10.1242/jcs.063875
- Li L, Zhou Y, Sun L, et al. NuSAP is degraded by APC/C-Cdh1 and its overexpression results in mitotic arrest dependent of its microtubules' affinity. *Cell Signal*. 2007;19(10):2046–2055. doi:10.1016/j.cellsig.2007.05.017
- Li H, Durbin R. Fast and accurate short read alignment with burrows-wheeler transform. *Bioinformatics*. 2009;25(14):1754–1760. doi:10.1093/bioinformatics/btp324
- McKenna A, Hanna M, Banks E, et al. The genome analysis toolkit: a MapReduce framework for analyzing next-generation DNA sequencing data. *Genome Res*. 2010;20(9):1297–1303. doi:10.1101/gr.107524.110
- Pais LS, Snow H, Weisburd B, et al. Seqr: a web-based analysis and collaboration tool for rare disease genomics. *Hum Mutat*. 2022;43(6):698–707. doi:10.1002/humu.24366
- Velmeshev D, Schirmer L, Jung D, et al. Single-cell genomics identifies cell type-specific molecular changes in autism. *Science*. 2019;364(6441):685–689. doi:10.1126/science.aav8130
- Zheng GX, Terry JM, Belgrader P, et al. Massively parallel digital transcriptional profiling of single cells. *Nat Commun*. 2017;8:14049. doi:10.1038/ncomms14049
- Satija R, Farrell JA, Gennert D, Schier AF, Regev A. Spatial reconstruction of single-cell gene expression data. *Nat Biotechnol*. 2015;33(5):495–502. doi:10.1038/nbt.3192
- (BICCN) BICCN. A multimodal cell census and atlas of the mammalian primary motor cortex. *Nature*. 2021;598(7879):86–102. doi:10.1038/s41586-021-03950-0



15. Sobreira N, Schiettecatte F, Valle D, Hamosh A. GeneMatcher: a matching tool for connecting investigators with an interest in the same gene. *Hum Mutat.* 2015;36(10):928-930. doi:10.1002/humu.22844
16. Ben-Shachar S, Khajavi M, Withers MA, et al. Dominant versus recessive traits conveyed by allelic mutations—to what extent is nonsense-mediated decay involved? *Clin Genet.* 2009;75(4):394-400. doi:10.1111/j.1399-0004.2008.01114.x
17. Hamanaka K, Imagawa E, Koshimizu E, et al. De novo truncating variants in the last exon of SEMA6B cause progressive myoclonic epilepsy. *Am J Hum Genet.* 2020;106(4):549-558. doi:10.1016/j.ajhg.2020.02.011
18. Karczewski KJ, Francioli LC, Tiao G, et al. The mutational constraint spectrum quantified from variation in 141,456 humans. *Nature.* 2020;581(7809):434-443. doi:10.1038/s41586-020-2308-7
19. Iyer J, Moghe S, Furukawa M, Tsai MY. What's Nu(SAP) in mitosis and cancer? *Cell Signal.* 2011;23(6):991-998. doi:10.1016/j.cellsig.2010.11.006
20. Nie J, Wang H, He F, Huang H. Nusap1 is essential for neural crest cell migration in zebrafish. *Protein Cell.* 2010;1(3):259-266. doi:10.1007/s13238-010-0036-8
21. Li C, Zhang Y, Yang Q, et al. NuSAP modulates the dynamics of kinetochore microtubules by attenuating MCAK depolymerisation activity. *Sci Rep.* 2016;6:18773. doi:10.1038/srep18773
22. Ozlü N, Monigatti F, Renard BY, et al. Binding partner switching on microtubules and aurora-B in the mitosis to cytokinesis transition. *Mol Cell Proteomics.* 2010;9(2):336-350. doi:10.1074/mcp.M900308-MCP200
23. Coban-Akdemir Z, White JJ, Song X, et al. Identifying genes whose mutant transcripts cause dominant disease traits by potential gain-of-function alleles. *Am J Hum Genet.* 2018;103(2):171-187. doi:10.1016/j.ajhg.2018.06.009

## SUPPORTING INFORMATION

Additional supporting information can be found online in the Supporting Information section at the end of this article.

**How to cite this article:** Mo A, Paz-Ebstein E, Yanovsky-Dagan S, et al. A recurrent de novo variant in *NUSAP1* escapes nonsense-mediated decay and leads to microcephaly, epilepsy, and developmental delay. *Clinical Genetics.* 2023;1-8. doi:10.1111/cge.14335